LETTER

doi:10.1038/nature10228

# Control of $T_H17$ cells occurs in the small intestine

Enric Esplugues[1,2,3]*, Samuel Huber[1,4]*, Nicola Gagliani[5], Anja E. Hauser[2], Terrence Town[6,7], Yisong Y. Wan[8], William O'Connor Jr[1], Anthony Rongvaux[1], Nico Van Rooijen[9], Ann M. Haberman[10], Yoichiro Iwakura[11], Vijay K. Kuchroo[12], Jay K. Kolls[13], Jeffrey A. Bluestone[14], Kevan C. Herold[1] & Richard A. Flavell[1,15]

**Interleukin (IL)-17-producing T helper cells ($T_H17$) are a recently identified $CD4^+$ T cell subset distinct from T helper type 1 ($T_H1$) and T helper type 2 ($T_H2$) cells[1]. $T_H17$ cells can drive antigen-specific autoimmune diseases and are considered the main population of pathogenic T cells driving experimental autoimmune encephalomyelitis (EAE)[2], the mouse model for multiple sclerosis. The factors that are needed for the generation of $T_H17$ cells have been well characterized[3–6]. However, where and how the immune system controls $T_H17$ cells *in vivo* remains unclear. Here, by using a model of tolerance induced by CD3-specific antibody, a model of sepsis and influenza A viral infection (H1N1), we show that pro-inflammatory $T_H17$ cells can be redirected to and controlled in the small intestine. $T_H17$-specific IL-17A secretion induced expression of the chemokine CCL20 in the small intestine, facilitating the migration of these cells specifically to the small intestine via the CCR6/CCL20 axis. Moreover, we found that $T_H17$ cells are controlled by two different mechanisms in the small intestine: first, they are eliminated via the intestinal lumen; second, pro-inflammatory $T_H17$ cells simultaneously acquire a regulatory phenotype with *in vitro* and *in vivo* immune-suppressive properties ($rT_H17$). These results identify mechanisms limiting $T_H17$ cell pathogenicity and implicate the gastrointestinal tract as a site for control of $T_H17$ cells.**

$T_H17$ cells have been associated with the pathogenesis of several chronic inflammatory disorders, including rheumatoid arthritis and multiple sclerosis[2,7]. To study the cellular and molecular mechanisms that control pathogenicity mediated by $T_H17$ cells we first used the CD3-specific antibody treatment model. It is known that CD3-specific antibody treatment induces a 'cytokine storm' and local inflammation mainly in the small intestine[8]. Despite this it has been validated as an *in vivo* model of tolerization[9] and is now under study in human clinical trials[10]. By mimicking antigen, CD3-specific antibody treatment leads to activation-induced cell death (AICD) of T cells[11,12] and consequently a systemic upregulation of IL-6 (ref. 9) and transforming growth factor-β (TGF-β1) induced by phagocyte engulfment of apoptotic T cells[13]. In line with these publications, we found that CD3-specific antibody treatment induced an immunoregulatory environment marked by simultaneous expression of TGF-β1 and IL-6 (Fig. 1a). The combination of these cytokines is important for the development of $T_H17$ cells *in vitro* and *in vivo* as it has been previously clearly established[3,4]. Accordingly, we found elevated levels of IL-17A in plasma of CD3-specific antibody-treated animals compared to controls (Fig. 1a).

First, we aimed to investigate the source of IL-17A. It has been reported that a few hours after injection of CD3-specific antibody, there is a rapid disappearance of the majority of T cells from the

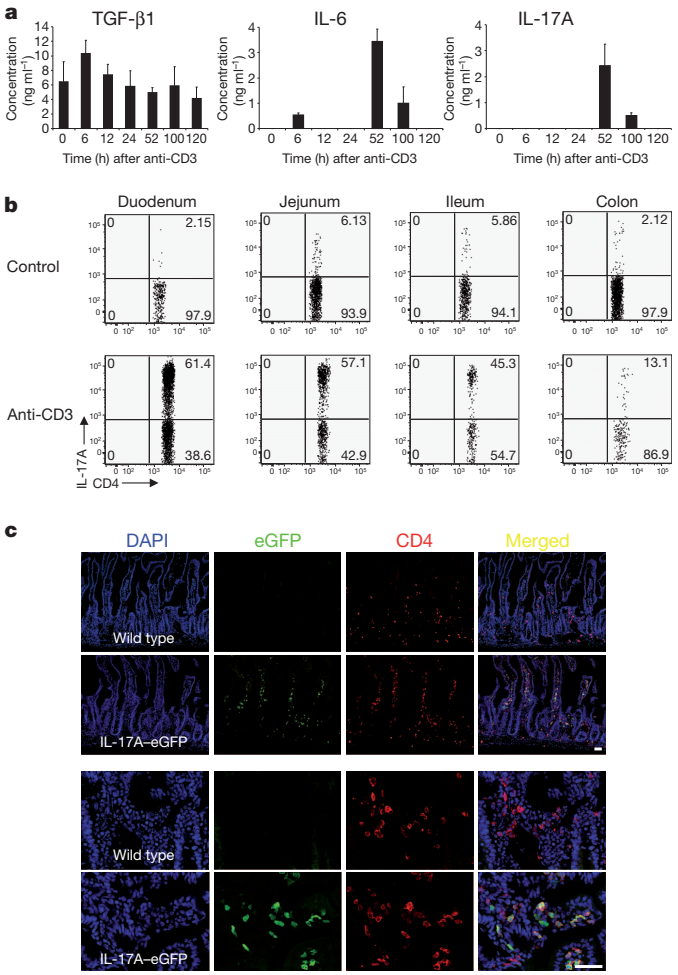


**Figure 1 | Accumulation of $T_H17$ cells in the small intestine after CD3-specific antibody treatment.** Mice were injected with CD3-specific antibody. **a**, Plasma levels of TGF-β1, IL-6 and IL-17A. Mean ± s.e.m.; $n = 4$. **b**, Flow cytometric analysis of IL-17A–eGFP expression (gated on $CD4^+TCR\beta^+$ events); numbers in quadrants indicate percent cells in each. **c**, Immunofluorescence staining of frozen sections of the small intestine after CD3-specific antibody treatment (eGFP, green; CD4, red; cell nuclei, DAPI). Scale bar, 50 μm. Data are representative of at least three independent experiments.

[1]Department of Immunobiology, Yale University School of Medicine, New Haven, Connecticut 06520, USA. [2]German Rheumatism Research Center (DRFZ), A Leibniz Institute, Berlin 10117, Germany. [3]Cluster of Excellence NeuroCure, Charite-Universitätsmedizin Berlin, Berlin 10117, Germany. [4]I. Medizinische Klinik, Universitätsklinikum Hamburg-Eppendorf, Hamburg 20246, Germany. [5]San Raffaele Diabetes Research Institute (HSR-DRI), Milan 20132, Italy. [6]Departments of Biomedical Sciences and Neurosurgery, Cedars-Sinai Medical Center, Los Angeles, California 90048, USA. [7]Department of Medicine, David Geffen School of Medicine, University of California, Los Angeles, California 90048, USA. [8]Lineberger Comprehensive Cancer Center, Department of Microbiology and Immunology, The University of North Carolina, School of Medicine, Chapel Hill, North Carolina 27599, USA. [9]Department of Molecular Cell Biology, Faculty of Medicine, Vrije Universiteit, Amsterdam, 1081 BT, The Netherlands. [10]Department of Laboratory Medicine, Yale University School of Medicine, New Haven, Connecticut 06520, USA. [11]Center for Experimental Medicine, Institute of Medical Science, University of Tokyo, Tokyo 108-8639, Japan. [12]Center for Neurologic Diseases, Brigham and Women's Hospital, Harvard Medical School, Boston, Massachusetts 02115, USA. [13]Department of Genetics, LSU Health Sciences Center, New Orleans, Louisiana 70112, USA. [14]Diabetes Center at the University of California San Francisco, San Francisco, California 94143, USA. [15]Howard Hughes Medical Institute, New Haven, *These authors contributed equally to this work.

circulation[13,14]. Surprisingly, in parallel with the disappearance of T cells from the periphery, we found a concomitant increase in the percentage and the number of total T cells in the small intestine, in particular in the duodenum (Supplementary Fig. 1a–c). In a newly generated IL-17A–eGFP knock-in mouse (enhanced green fluorescent protein was inserted in the *Il17a* locus; Methods and Supplementary Fig. 2a–d and 3a–c) injected with CD3-specific antibody, 50–80% of the $CD4^+TCR\beta^+$ T cells located in the duodenum were expressing IL-17A (Fig. 1b and Supplementary Fig. 1d, e). The percentage and number of $T_H17$ cells in the intestine decreased from the duodenum to the colon in a gradient-like fashion (Fig. 1b). Detection of $CD4^+eGFP^+$ T cells by immunofluorescence and two-photon-laser-scanning microscopy confirmed the high frequency of $T_H17$ cells in the small intestine *in situ* (Fig. 1c and Supplementary Fig. 4a–c). Importantly, we also found $T_H17$ cell infiltration in the duodenum when animals were injected with a therapeutic non-FcR-binding CD3-specific antibody[15], although the frequency and numbers of the $T_H17$ cells were lower compared to the FcR-binding antibody (Supplementary Fig. 5a). Similar results were observed after antigen-specific stimulation when soluble myelin oligodendrocyte glycoprotein antigen (MOG) was administered to MOG-TCR transgenic mice (2D2 mice)[16] (Supplementary Fig. 5b). Taken together these data suggest that the generation and the accumulation of $T_H17$ cells in the small intestine was not restricted to the CD3-specific antibody treatment, but was a general mechanism following strong T-cell receptor (TCR) stimulation.

We next wanted to identify the molecular signals important for the generation of $T_H17$ cells *in vivo* after CD3-specific antibody treatment. Because IL-6 is known to be important for $T_H17$ cell generation, we evaluated the importance of this cytokine. *Il6*$^{-/-}$ and wild-type mice were treated with CD3-specific antibody. In the *Il6*$^{-/-}$ mice, only a very small population of $T_H17$ cells (about 2%) could be found by flow cytometry in the small intestine (Supplementary Fig. 6a) and IL-17A was undetectable in the plasma (data not shown). To study the cellular source of IL-6, we treated mice with clodronate-loaded liposomes, which eliminates most macrophages and a significant proportion of dendritic cells compared to PBS-loaded liposomes[13] (Supplementary Fig. 6c). IL-6 plasma levels were greatly reduced in mice treated with clodronate-loaded liposomes compared to control mice after CD3-specific antibody injection (Supplementary Fig. 6d) and a profound reduction in $T_H17$ cells was observed (Supplementary Fig. 6b, c). Taken together, these data support the notion that IL-6 secreted by antigen-presenting cells (APCs) is critical for the generation of $T_H17$ cells during CD3-specific antibody treatment.

We next analysed the mechanism leading to the specific accumulation of $T_H17$ cells in the small intestine, predominantly in the duodenum. $T_H17$ cells are known to express the chemokine receptor CCR6 (ref. 17). Whereas CCR6 is relevant in different autoimmune disease models[7,18], the role of the CCR6/CCL20 axis in immune cell migration to the intestine during tolerance induction has not yet been evaluated. To study that, we analysed the expression of CCR6 on $CD4^+$ IL-17A–eGFP positive and negative cells (Fig. 2a) and *Ccl20* mRNA expression (Fig. 2b) in the spleen and the gut. CCR6 was mainly expressed in $T_H17$ cells from the spleen and the gut 24 h after CD3-specific antibody injection (Fig. 2a). Strikingly, when we performed a time course to measure the mRNA levels of *Ccl20* in different parts of the intestine during CD3-specific antibody treatment, we observed that *Ccl20* was expressed at the highest level in the duodenum in steady state conditions and was selectively further upregulated after CD3-specific antibody treatment (Fig. 2b, c and Supplementary Fig. 7). To test the importance of the CCR6/CCL20 axis for the migration of $T_H17$ cells from the periphery to the duodenum, we treated *Ccr6*$^{-/-}$ and control mice with CD3-specific antibody. $T_H17$ cell number (Fig. 2e) and frequency (Fig. 2d) were strongly reduced in the intestine of the *Ccr6*$^{-/-}$ compared to wild-type mice. In general, we did not observe signs of intestinal inflammation in the *Ccr6*$^{-/-}$ mice as we did

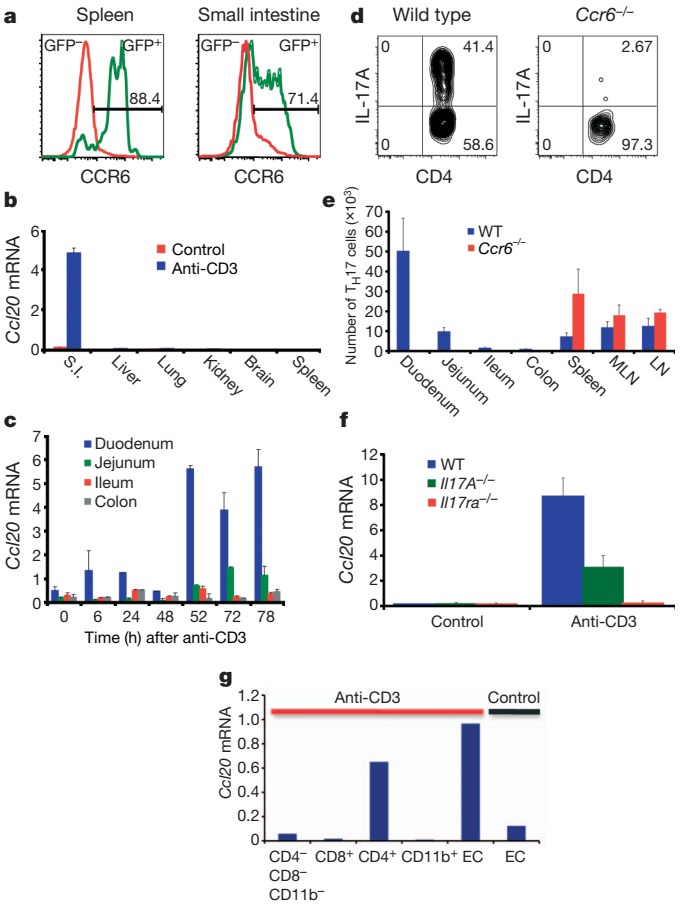


**Figure 2 | The axis CCR6/CCL20 is essential for the recruitment of $T_H17$ cells to the small intestine.** **a**, CCR6 expression 24 h after anti-CD3 treatment. **b**, **c**, *Ccl20* mRNA expression (mean ± s.e.m.; $n = 4$). S.I., small intestine. **d**, IL-17A expression (gated on $CD4^+TCR\beta+$ events) as measured by intracellular cytokine staining. **e**, $T_H17$ cell numbers in different organs (mean ± s.d.; $n = 5$). LN, lymph node; MLN, mesenteric lymph node. **f**, *Ccl20* mRNA expression in duodenum of wild-type (WT), *Il17a*$^{-/-}$ and *Il17ra*$^{-/-}$ mice (mean ± s.e.m.;$n = 4$). **g**, *Ccl20* mRNA levels of epithelial and haematopoietic cells isolated from the small intestine. EC, epithelial cells. Panels **b**, **d**–**g** show results 100 h after the first anti-CD3 injection. Data are representative of at least three independent experiments.

in wild-type controls after CD3-specific antibody treatment (data not shown). Interestingly, we detected a higher number of $T_H17$ cells in the spleen and lymph nodes of *Ccr6*$^{-/-}$ mice when compared to control animals (Fig. 2e). This increase was accompanied by splenomegaly and enlargement of lymph nodes (data not shown), indicating that CCR6 does not have a major role in the generation and expansion of $T_H17$ cells. In conclusion, CCR6 seems to be essential for the migration of $T_H17$ cells to the small intestine after CD3-specific antibody treatment, and the intestinal inflammation is dependent on this migration. Thus our data indicate that $T_H17$ cell migrate to the small intestine leading to intestinal inflammation and damage. However, we cannot exclude that a proliferation of gut resident $T_H17$ cells also contributes to the observed phenomenon.

To evaluate the contribution of IL-17A and IL-17F ($T_H17$ signature cytokines) in the induction of CCL20 expression in the duodenum, we treated *Il17a*$^{-/-}$ or *Il17ra*$^{-/-}$ mice with CD3-specific antibody. We found decreased levels of CCL20 in the *Il17a*$^{-/-}$ and the *Il17ra*$^{-/-}$ mice versus the controls after CD3-specific antibody treatment (Fig. 2f), indicating that IL-17 signalling has a major role in the induction of CCL20 in the duodenum. We next studied the cellular source of CCL20. *Ccl20* mRNA was only detectable in the intestinal epithelial cells in untreated mice. Treatment with CD3-specific antibody led to a

further upregulation of *Ccl20* mRNA by the epithelial cells. Additionally, the $CD4^+$ T cells present in the small intestine after CD3-specific antibody treatment, most of which were $T_H17$ cells, expressed high levels of *Ccl20* mRNA (Fig. 2g). In conclusion, $T_H17$ cells via IL-17A and IL-17F production directly upregulate CCL20 production by the intestinal epithelial cells, which then leads to the subsequent recruitment of $CCR6^+$ $T_H17$ cells, which also produce CCL20.

Of note, the intestinal inflammation after CD3-specific antibody treatment was transient and 100% of the mice recovered. To understand better the mechanisms underlying this process, we first assessed apoptosis of $T_H17$ cells in the small intestine but we did not detect a significant number of apoptotic cells (data not shown). When we studied the *in vivo* proliferation capacity of $CD4^+TCR\beta^+$ T cells from the CD3-specific antibody-treated animals, we found that $T_H17$ cells from the duodenum were actively proliferating (Supplementary Figs 8 and 9a, b). Using IL17A–eGFP × FoxP3–mRFP double reporter mice (monomeric red fluorescent protein was inserted in the *foxp3* locus) we determined that $CD4^+$IL-$17A^+$ T cells were proliferating at a higher rate than $CD4^+$IL-$17A^-$ T cells in the duodenum (Supplementary Figs 8 and 9). Using two-photon laser-scanning microscopy, we found that the $T_H17$ cells in the duodenum did not show the typical behaviour of an apoptotic T cell, conversely, they behaved like activated T cells in terms of their pattern of speed and direction of migration (Supplementary Video). Taken together these data indicate that $T_H17$ cells do not die in the small intestine, but are rather actively proliferating.

In line with previous publications[8] we found that CD3-specific antibody treatment caused diarrhoea, oedema, inflammation and tissue destruction in the small intestine (Supplementary Fig. 10a, b), which correlated with the recruitment of $T_H17$ cells. However, the intestinal pathology was only transient and mice fully recovered. We therefore began to investigate the fate of $T_H17$ cells in the small intestine. Interestingly, we found a fraction of $T_H17$ cells in the intestinal lumen

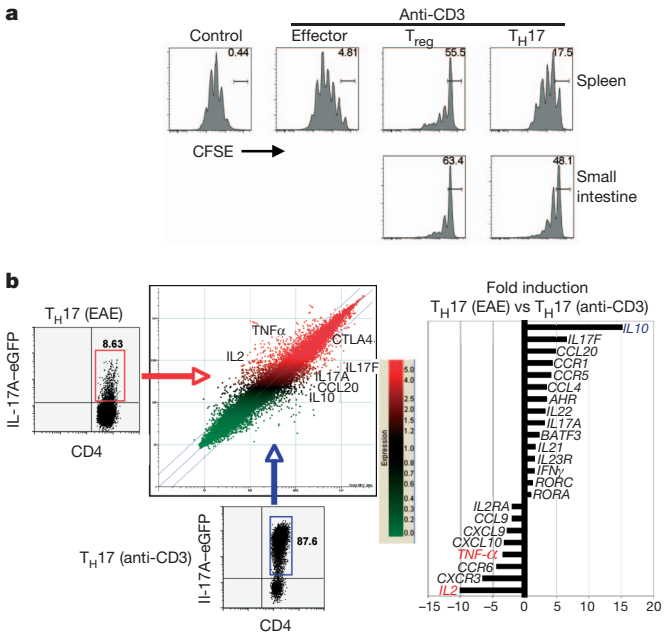


**Figure 3 | Functional and molecular characterization of $rT_H17$ cells.** **a**, Suppression assay was performed using $eGFP^-mRFP^-CD4^+$ (Effector), $eGFP^-mRFP^+CD4^+$ (Tregs) or $eGFP^+mRFP^-CD4^+$ ($T_H17$) cells sorted from spleen or small intestine. (Bar represents undivided CFSE-labelled $CD4^+CD25^-$ responder T cells). Data are representative of six independent experiments. **b**, Gene expression analysis comparing $T_H17$ cells ($eGFP^+mRFP^-CD4^+$) from central nervous system at day 17 after EAE induction versus $T_H17$ cells isolated from the small intestine of anti-CD3 treated IL-17A–eGFP × Foxp3–mRFP double reporter mice.

of the CD3-specific antibody-treated mice (Supplementary Fig. 10c, d). Given the severe inflammation, diarrhoea and tissue damage (Supplementary Fig. 10a, b), it is most likely that these cells were passively washed out, although an active mechanism cannot be excluded. Considering that the remaining $T_H17$ cells in the duodenum were actively proliferating, but the intestinal pathology was only transient, we were curious about the functional capabilities of these cells. Surprisingly, we found that the remaining $T_H17$ cells in the duodenum were able to suppress proliferation of responder T cells *in vitro* (Fig. 3a). To study the molecular properties of these suppressive $T_H17$ cells (which we refer from now on as $rT_H17$ cells), we performed a genome-wide transcriptional profiling assay (Fig. 3b). We compared the gene expression pattern of $rT_H17$ cells from CD3-specific antibody-treated mice and genes expressed by pro-inflammatory $T_H17$ cells that were harvested from the central nervous system of EAE-induced mice. The signature genes of $T_H17$ cells, like *Rorc*, *Rora*, *Il17a*, *Il22* or *Il23r*, were similarly expressed between both types of $T_H17$ cells. Also the activation status of these cells seemed to be similar, because activation markers such as CD69, CD25 and CD44 were equally expressed. However, we found that the $rT_H17$ cells from the CD3-specific antibody-treated mice showed a non-inflammatory gene expression profile compared to pro-inflammatory $T_H17$ cells isolated from the central nervous system of EAE-induced mice. Notably, the expression levels of *Tnf-α* and *Il-2*, two cytokines with clear pro-inflammatory roles[19,20], were greatly reduced in the $rT_H17$ cells from the small intestine. In contrast, these cells expressed high levels of IL-10, a cytokine with potent anti-inflammatory activities[21] (Supplementary Fig. 11b and Fig. 3b). These data are supported by a previous report showing that *in-vitro*-generated non-pathogenic $T_H17$ cells are able to express IL-10 (ref. 22). To evaluate the molecular mechanisms involved in the suppressive function of the $rT_H17$ cells, different molecules were blocked in an *in vitro* suppression assay using monoclonal antibodies (Supplementary Fig. 11a). The suppressive capacity of the $rT_H17$ cells was partially dependent on IL-10, CTLA-4 and TGF-β. Blocking all three pathways resulted in a lack of suppression by the $rT_H17$ cells. $T_H17$ cells isolated from the spleen showed an intermediate phenotype. They exhibited a limited capacity to suppress the proliferation of T cells *in vitro* (Fig. 3a), and also produced more TNF-α and IL-2, but less IL-10 compared to $T_H17$ cells isolated from the small intestine (Supplementary Fig. 11b). However, because some of the $T_H17$ cells in the small intestine downregulated CCR6 (Fig. 2a), it is possible that some $rT_H17$ might have migrated back from the small intestine to the spleen. If development of the suppressive capability occurred in the small intestine, then preventing the migration of the $T_H17$ cells to that site should prevent the development of these tolerogenic cells. To test this hypothesis, we analysed $T_H17$ cells isolated from the spleen of $Ccr6^{-/-}$ mice, because we showed already that these $T_H17$ cells are unable to migrate to the small intestine. Consistent with the hypothesis, $Ccr6^{-/-}$ $T_H17$ cells in the spleen showed high TNF-α production, failed to suppress T-cell proliferation *in vitro*, and were even proinflammatory, causing inflammatory bowel disease *in vivo* upon transfer into a lymphopenic host (Supplementary Fig. 12 a–d). These data indicate that proinflammatory $T_H17$ cells do indeed acquire their suppressive phenotype in the small intestine.

To confirm our findings in an animal disease model, EAE-induced mice were treated with CD3-specific antibody. In line with a previous publication[23] we observed a protective effect when the treatment was administered during the course of the disease (Supplementary Fig. 13a). More importantly, we demonstrated that $T_H17$ cells were recruited to the duodenum of the CD3-specific antibody treated animals and these mice had strongly reduced numbers of $T_H17$ cells in the central nervous system (data not shown). Using a MOG-specific tetramer, we determined that a significant percentage of $T_H17$ cells in the duodenum were antigen-specific (Supplementary Fig. 13b), demonstrating that MOG-specific $T_H17$ cells were recruited to the duodenum following CD3-specific antibody treatment. In contrast the frequency

of MOG-tetramer-positive $T_H17$ cells was much lower in other organs of EAE-induced mice, which had not been treated with CD3-specific antibody (data not shown). This is evidence against a general increase in MOG-specific $T_H17$. Therefore our results show that antigen-specific $T_H17$ cells, with proinflammatory properties, generated in the periphery can be redirected to the small intestine. To confirm that $rT_H17$ cells isolated from the small intestine of CD3-specific antibody-treated mice are indeed *in vivo* immune-suppressive we tested their suppressive capacity in an EAE transfer model. We co-transferred MOG-specific *in-vitro*-differentiated $T_H17$ either alone or together with MOG-specific $rT_H17$ cells isolated from the small intestine of CD3-specific antibody-treated 2D2 transgenic mice. Strikingly, we found that $rT_H17$ cells were able to completely suppress the development of EAE in these transfer experiments (Supplementary Fig. 13c, d), indicating that the $rT_H17$ cells are indeed stable in terms of their immune suppressive function.

As mentioned above CD3-specific antibody treatment is already used in clinical trials[9,10], and we therefore aimed to confirm our results using teplizumab (hOKT3γ1(Ala-Ala)), one CD3-specific antibody used in these trials. To that end we used a humanized mouse system: we reconstituted Balb/c Rag-$2^{-/-}\gamma c^{-/-}$ double knockout mice with human peripheral blood mononuclear cells. Two weeks after the transfer we treated these mice with either OKT-3, an FcR-binding CD3-specific antibody used in the first human studies, or teplizumab, an FcR non-binding CD3-specific antibody. Strikingly, we found human T cells in the small intestine after treatment with both of these CD3-specific antibodies (Supplementary Fig. 14a, b). The presence of human IL-17A-, IL-10- and CCL20-producing cells in the small intestine in OKT-3- and teplizumab-treated mice was confirmed by real-time PCR (Supplementary Fig. 14c).

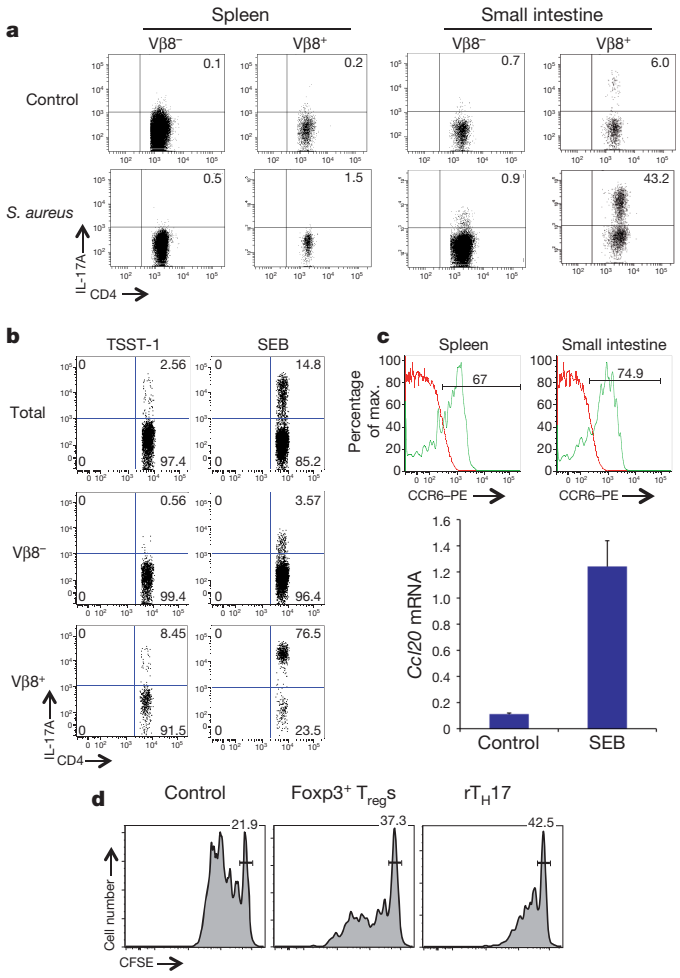


**Figure 4 | $T_H17$ cells are recruited to the small intestine during sepsis.** **a**, **b**, IL-17A–eGFP expression is shown (gated on $CD4^+TCR\beta^+$ events). Mice were injected with *Staphylococcus aureus* (**a**) or SEB and TSST-1 (**b**). **c**, CCR6 expression 24 h after the first SEB injection (top). *Ccl20* mRNA levels in the small intestine 100 h after the first injection (mean ± s.e.m.; $n = 4$) (bottom). **d**, *In vitro* suppression assay using $CD4^+$IL-17A–$eGFP^+$ cells from the small intestine or $CD4^+$Foxp3–$mRFP^+$ cells from the spleen of SEB-treated mice as suppressor cells. Results are representative of at least two independent experiments.

$T_H17$ cells have a crucial role in controlling different microorganisms *in vivo*[24]. We next investigated whether this mechanism of $T_H17$ cell control also functions during a strong immune response elicited by pathogenic microorganisms. We first used a murine model of sepsis. We injected *Staphylococcus aureus*, which is one of the most frequent organisms responsible for sepsis in humans[25,26], intravenously into IL-17A–eGFP reporter mice. Mice were analysed 3 days after the injection, at a time when they displayed severe clinical symptoms of sepsis (weight loss, dehydration, lethargy). Strikingly, we found the highest frequency and number of $T_H17$ in the small intestine (Fig. 4a). Interestingly, most $T_H17$ appeared to be TCR $V\beta8^+$. The injection of the superantigen SEB (*Staphylococcus aureus* enterotoxin B), which is produced by the bacteria used in these experiments and binds to $V\beta8^+$ T cells, was sufficient to induce the accumulation of $T_H17$ in the small intestine just as in the anti-CD3 studies. As a control we injected mice with TSST-1 (toxic shock syndrome toxin 1), a superantigen that does not bind to Vβ8 and is not produced by the bacteria we used. Of note, we observed that the administration of TSST-1 was less effective at inducing the accumulation of $T_H17$ cells in the small intestine (Fig. 4b). Finally, we could confirm that the $T_H17$ cells, induced by SEB treatment, expressed CCR6 and that CCL20 is specifically upregulated in the small intestine following SEB treatment (Fig. 4c). Furthermore, while a subpopulation of the $T_H17$ cells was found in the intestinal lumen (Supplementary Fig. 15), the remaining $T_H17$ cells demonstrated an immune-suppressive phenotype (Fig. 4d and Supplementary Fig. 16), again comparable to our results obtained in the CD3-specific antibody treatment. Interestingly, it is known that SEB can induce tolerance[27], which is in line with our results that SEB leads to the generation of $rT_H17$ cells. Accordingly, we found that SEB and, to a lesser extent, TSST-1 treatment of EAE-induced mice led to the amelioration of disease (data not shown), which is in line with one previous publication[28].

In addition to anti-bacterial immunity, viruses are the next key class of pathogens to which we must respond, yet contain excessive immunopathology which is commonly the cause of morbidity and mortality[29]. To address such an immune response, we analysed influenza, a viral infection that has devastated human populations. Notably, we again found increased $T_H17$ cell frequencies in the small intestine in mice infected with influenza A (H1N1) (Supplementary Fig. 17).

In conclusion, we propose a general mechanism that could explain how a pro-inflammatory $T_H17$ immune response, which is beneficial in clearing infection, but immunopathogenic in excess, can be controlled by the mechanisms we describe here: namely by acquisition of an immune-suppressive phenotype or elimination into the intestinal lumen (Supplementary Fig. 18). These findings and further studies aiming to identify the underlying mechanism of the conversion of pro-inflammatory $T_H17$ cells into $rT_H17$ cells may help in designing new strategies to control auto-reactive $T_H17$ cells in autoimmune diseases like multiple sclerosis.

## METHODS SUMMARY

**Anti-CD3, SEB, TSST-1 treatment and *Staphylococcus aureus* infection.** Mice were injected intraperitoneally three times with either CD3-specific antibody

(clone 2C11, 20 μg per mouse) SEB (50 μg per mouse) or TSST-1 (50 μg per mouse) at 0, 48 and 96 h. Mice were analysed 100 h after the first injection, if not otherwise specified. *Staphylococcus aureus* was injected intravenously ($1 \times 10^8$ colony-forming units per mouse) in order to induce sepsis. Mice were killed 3 days after the injection.

**Flow cytometric analysis.** Cells were isolated from the organ as indicated. IL-17A–eGFP and CCR6 expression was assessed directly after isolation. When indicated cells were restimulated and intracellular cytokine staining for IL-17A was performed. Numbers in dot-plot quadrants indicate percent cells in each. Cells were gated on $CD4^+TCR\beta^+$ events.

**Real-time PCR.** *Ccl20* mRNA expression was measured in different tissues as indicated using real time PCR with reverse transcription.

***In vitro* suppression assay.** Different suppressor cells were co-cultured with carboxyfluorescein diacetate succinimidyl ester (CFSE)-labelled $CD4^+CD25^-$ responder T cells, which were isolated from the spleen of CD45.1 congenic mice. Bar represents undivided CFSE-labelled responder T cells.

**Full Methods** and any associated references are available in the online version of the paper at www.nature.com/nature.

**Received 12 May 2010; accepted 19 May 2011.**
**Published online 17 July 2011.**

1. Korn, T., Bettelli, E., Oukka, M. & Kuchroo, V. K. IL-17 and Th17 cells. *Annu. Rev. Immunol.* **27,** 485–517 (2009).
2. Langrish, C. L. *et al.* IL-23 drives a pathogenic T cell population that induces autoimmune inflammation. *J. Exp. Med.* **201,** 233–240 (2005).
3. Bettelli, E. *et al.* Reciprocal developmental pathways for the generation of pathogenic effector $T_H17$ and regulatory T cells. *Nature* **441,** 235–238 (2006).
4. Mangan, P. R. *et al.* Transforming growth factor-β induces development of the $T_H17$ lineage. *Nature* **441,** 231–234 (2006).
5. Manel, N., Unutmaz, D. & Littman, D. R. The differentiation of human $T_H$-17 cells requires transforming growth factor-β and induction of the nuclear receptor RORγt. *Nature Immunol.* **9,** 641–649 (2008).
6. Yang, L. *et al.* IL-21 and TGF-β are required for differentiation of human $T_H17$ cells. *Nature* **454,** 350–352 (2008).
7. Hirota, K. *et al.* Preferential recruitment of CCR6-expressing Th17 cells to inflamed joints via CCL20 in rheumatoid arthritis and its animal model. *J. Exp. Med.* **204,** 2803–2812 (2007).
8. Merger, M. *et al.* Defining the roles of perforin, Fas/FasL, and tumour necrosis factor α in T cell induced mucosal damage in the mouse intestine. *Gut* **51,** 155–163 (2002).
9. Chatenoud, L. & Bluestone, J. A. CD3-specific antibodies: a portal to the treatment of autoimmunity. *Nature Rev. Immunol.* **7,** 622–632 (2007).
10. Herold, K. C. *et al.* Treatment of patients with new onset type 1 diabetes with a single course of anti-CD3 mAb teplizumab preserves insulin production for up to 5 years. *Clin. Immunol.* **132,** 166–173 (2009).
11. Carpenter, P. A. *et al.* Non-Fc receptor-binding humanized anti-CD3 antibodies induce apoptosis of activated human T cells. *J. Immunol.* **165,** 6205–6213 (2000).
12. Smith, C. A., Williams, G. T., Kingston, R., Jenkinson, E. J. & Owen, J. J. Antibodies to CD3/T-cell receptor complex induce death by apoptosis in immature T cells in thymic cultures. *Nature* **337,** 181–184 (1989).
13. Perruche, S. *et al.* CD3-specific antibody-induced immune tolerance involves transforming growth factor-β from phagocytes digesting apoptotic T cells. *Nature Med.* **14,** 528–535 (2008).
14. Chatenoud, L., Primo, J. & Bach, J. F. CD3 antibody-induced dominant self tolerance in overtly diabetic NOD mice. *J. Immunol.* **158,** 2947–2954 (1997).
15. Alegre, M. L. *et al.* An anti-murine CD3 monoclonal antibody with a low affinity for Fc gamma receptors suppresses transplantation responses while minimizing acute toxicity and immunogenicity. *J. Immunol.* **155,** 1544–1555 (1995).
16. Bettelli, E. *et al.* Myelin oligodendrocyte glycoprotein-specific T cell receptor transgenic mice develop spontaneous autoimmune optic neuritis. *J. Exp. Med.* **197,** 1073–1081 (2003).
17. Annunziato, F. *et al.* Phenotypic and functional features of human Th17 cells. *J. Exp. Med.* **204,** 1849–1861 (2007).
18. Reboldi, A. *et al.* C-C chemokine receptor 6-regulated entry of $T_H$-17 cells into the CNS through the choroid plexus is required for the initiation of EAE. *Nature Immunol.* **10,** 514–523 (2009).
19. Brown, S. J. & Mayer, L. The immune response in inflammatory bowel disease. *Am. J. Gastroenterol.* **102,** 2058–2069 (2007).
20. Petitto, J. M., Streit, W. J., Huang, Z., Butfiloski, E. & Schiffenbauer, J. Interleukin-2 gene deletion produces a robust reduction in susceptibility to experimental autoimmune encephalomyelitis in C57BL/6 mice. *Neurosci. Lett.* **285,** 66–70 (2000).
21. Pestka, S. *et al.* Interleukin-10 and related cytokines and receptors. *Annu. Rev. Immunol.* **22,** 929–979 (2004).
22. McGeachy, M. J. *et al.* TGF-β and IL-6 drive the production of IL-17 and IL-10 by T cells and restrain $T_H$-17 cell-mediated pathology. *Nature Immunol.* **8,** 1390–1397 (2007).
23. Kohm, A. P. *et al.* Treatment with nonmitogenic anti-CD3 monoclonal antibody induces $CD4^+$ T cell unresponsiveness and functional reversal of established experimental autoimmune encephalomyelitis. *J. Immunol.* **174,** 4525–4534 (2005).
24. Khader, S. A., Gaffen, S. L. & Kolls, J. K. Th17 cells at the crossroads of innate and adaptive immunity against infectious diseases at the mucosa. *Mucosal Immunol.* **2,** 403–411 (2009).
25. Rodriguez-Creixems, M. *et al.* Bloodstream infections: evolution and trends in the microbiology workload, incidence, and etiology, 1985–2006. *Medicine (Baltimore)* **87,** 234–249 (2008).
26. Martin, G. S., Mannino, D. M., Eaton, S. & Moss, M. The epidemiology of sepsis in the United States from 1979 through 2000. *N. Engl. J. Med.* **348,** 1546–1554 (2003).
27. Ochi, A., Yuh, K. & Migita, K. Not every superantigen induces tolerance *in vivo*. *Semin. Immunol.* **5,** 57–63 (1993).
28. Soos, J. M., Schiffenbauer, J. & Johnson, H. M. Treatment of PL/J mice with the superantigen, staphylococcal enterotoxin B, prevents development of experimental allergic encephalomyelitis. *J. Neuroimmunol.* **43,** 39–43 (1993).
29. Chowell, G. *et al.* Severe respiratory disease concurrent with the circulation of H1N1 influenza. *N. Engl. J. Med.* **361,** 674–679 (2009).

**Supplementary Information** is linked to the online version of the paper at www.nature.com/nature.

**Acknowledgements** The authors would like to thank F. Manzo for expert administrative assistance, L. Evangelisti and C. Hughes for generating embryonic stem cells and chimaeric mice, respectively, J. Stein for initial screening of knock-in mice, T. Ferrandino for assistance with the mouse colony, E. Eynon and J. Alderman for managing the mouse program and A. Lin for assistance with Gene Array analysis. We also thank T. Taylor and G. Tokmoulina for expert help with the FACS sorting and D. Gonzalez for help with the multiphoton microscopy. We would like to thank J. P. Allison for providing the anti-CTLA-4 antibody, F. Waldron-Lynch and J. S. Pober for providing peripheral blood mononuclear cells, and the NIH Tetramer core facility for providing the tetramers. W.O. was supported by a fellowship from the National Multiple Sclerosis Society. S.H. was supported by the DFG (HU 1714/1-1) and by a James Hudson Brown–Alexander B. Coxe Fellowship. E.E. was supported by the Spanish Ministry of Science postdoctoral fellowship and by a James Hudson Brown–Alexander B. Coxe Fellowship. R.A.F. is an Investigator of the Howard Hughes Medical Institute. The generation of mice for this work was supported by the Transgenic Core of the Yale DERC DK45735 and some of the work supported by a Pilot project from DK45735. This work was also supported by the JDRF.

**Author Contributions** E.E., S.H. and R.A.F. designed the study and wrote the manuscript; N.G. did the *in vitro* suppression assays and the flow analysis for IL-10 expression; A.E.H. and A.M.H did the two-photon laser-scanning microscopy experiments; T.T. did the immunohistochemistry analysis; W.O. supported the work with key suggestions and by editing the manuscript; E.E. and S.H. did all other *in vitro* and *in vivo* experimental work; Y.Y.W. provided Foxp3–mRFP mice; A.R. did the viral infection experiments; N.V.R. provided clodronate-loaded liposomes, V.K.K provided 2D2 mice and feedback on the manuscript; Y.I. provided *Il17a*$^{-/-}$ mice and feedback on the manuscript; J.K.K. provided the *Il17ra*$^{-/-}$ mice and feedback on the manuscript and J.A.B. provided CD3-specific antibodies and feedback on the manuscript; K.C.H. provided teplizumab and key suggestions. E.E. and R.A.F. co-directed the project.

**Author Information** Reprints and permissions information is available at www.nature.com/reprints. The authors declare no competing financial interests. Readers are welcome to comment on the online version of this article at www.nature.com/nature. Correspondence and requests for materials should be addressed to E.E. (enric.esplugues@yale.edu) or R.A.F. (richard.flavell@yale.edu).

## METHODS

**Mice.** BALB/c mice (blastocyst donors), CD1 mice (foster mothers), Tet-Cre transgenic mice ("deletor" mice, C57BL/6 background), C57BL/6 mice (B6), C57BL/6.Ly5.1 mice (CD45.1$^+$), *IL6*$^{-/-}$ mice and *CCR6*$^{-/-}$ mice were purchased from The Jackson Laboratories. MOG-transgenic mice (2D2 mice, C57BL/6 background)[30] and Foxp3 reporter mice (FIR mice, C57BL/6 background)[31] were intercrossed with the IL-17A–eGFP reporter mice. We also used *Il17a*$^{-/-}$, *Il17ra*$^{-/-}$ and IL-10–eGFP mice (Tiger mice)[32–34]. All mice were kept under specific pathogen-free conditions in the animal care facility at Yale University. The mice were studied at 6–12 week of age. All the experiments were approved by the Institutional Animal Care and Use Committee of Yale University.

**Generation of IL-17A–IRES–eGFP reporter mice.** A BAC clone consisting of *Il17a* genomic DNA derived from C57BL/6 mice was purchased from BacPac (Oakland, CA). An 8-kb BamHI–MluI fragment comprising exons 1, 2 and 3 for the *Il17a* gene was cloned into pEasy-Flox vector adjacent to the thymidine kinase selection marker. The internal ribosome entry site (IRES)–eGFP cassette was linked to a LoxP-flanked neomycin (Neo) selection marker to obtain the IRES–eGFP–Neo cassette. The targeting construct was generated by cloning the IRES–eGFP–Neo cassette into a SacII site between the translation stop codon (UGA) and the polyadenylation signal (A2UA3) of the *Il17a* gene. The targeting construct was linearized by ClaI cleavage and subsequently electroporated into Bruce4 C57BL/6 embryonic stem (ES) cells. Transfected ES cells were selected in the presence of 300 μg ml$^{-1}$ G418 and 1 μM ganciclovir. Drug-resistant ES cell clones were screened for homologous recombination by PCR. To obtain chimaeric mice, correctly targeted ES clones were injected into BALB/c blastocysts, which were then implanted into CD1 pseudopregnant foster mothers. Male chimaeras were bred with C57BL/6 to screen for germ-line transmitted offspring. Germ-line transmitted mice were bred with germline Cre transgenic mice (Tet-Cre mice) to remove the neomycin gene. Mice bearing the targeted *Il17a* allele were screened by PCR (*Il17a* knock-in (KI) sense: 5′-CACCAGCGCTGTGTCAAT-3′, *Il17a* KI anti-sense: 5′-ACAAACACGAAGCAGTTTGG-3′ and *Il17a* IRES: 5′-ACCGGCCTTATTCCAAGC-3′).

**Antibodies, tetramers and intracellular cytokine staining.** Anti-CD4 (L3T4), anti-CD62L (MEL-14), anti-CD44 (IM7), anti-CD45.1 (A20) and anti-CD45.2 (104), anti-TCRβ, anti-IL-2, anti-IL-17A, anti-TNFα, anti-Ki-67 and anti-BrdU (5′-bromo-2-deoxyuridine) were purchased from Becton Dickinson Pharmingen. For intracellular cytokine staining, the cells were restimulated with phorbol 12-myristate 13-acetate (PMA) (Sigma, 20 ng ml$^{-1}$) and ionomycin (Sigma, 0.5 μg ml$^{-1}$) for 4 h. Golgistop (BD Bioscience) was added during the last 3 h of restimulation. After restimulation, the cells were washed and a Ficoll gradient was performed. The cells were fixed with 1% paraformaldehyde (electron microscopy grade) for 10 min on ice. After two washes, cells were incubated with FITC-conjugated anti-GFP antibody (Rockland) and phycoerythrin (PE)-conjugated anti-IL-17A (BD Bioscience) in wash/perm solution (BD Bioscience) for 30 min on ice. Cells were washed twice and resuspended in PBS. Acquisitions were made with a LSRII cytometer (BD Bioscience).

For *ex vivo*-staining with $MOG_{38-49}$/I-A(b)-tetramer-allophycocyanin (APC)-labelled (mouse myelin oligodendrocyte glycoprotein 38-49, "GWYRSPFSRWH", NIH Tetramer Facility), single-cell suspensions were incubated at a density of $10^7$ cells ml$^{-1}$ with neuraminidase (0.7 μU ml$^{-1}$, neuraminidase type X from *Clostridium perfringens*, Sigma) in serum-free DMEM at 37 °C/10% $CO_2$ for 25 min before incubation with the I-A(b) multimers (30 μg ml$^{-1}$) in DMEM supplemented with 2% FCS (pH 8.0) at room temperature for 4 h. After washing, cells were stained for 7-AAD (Molecular Probes), CD4 (RM4-5) and TCRβ. hCLIP/I-A(b)-tetramer-APC-labelled was used as a control ("PVSKMRMATPLLMQA", NIH Tetramer Facility). The percentage of tetramer cells was determined in the CD4/TCRβ gate of live (7-AAD$^-$) cells. Stained cells were analysed on LSRII cytometer (BD Bioscience) and data were analysed with FlowJo software (Treestar).

**Flow cytometry and FACS sorting.** Collected lymphocytes were treated with ammonium chloride lysis buffer (BioSource International) to remove red blood cells and washed with RPMI containing 10% FBS (Gemini Biological Products). Cells were then stained with a 1:400 dilution of the indicated antibodies together with 10 μg ml$^{-1}$ anti-Fc-Receptor blocking antibody (2.4G2, American Type Culture Collection) in PBS containing 2% FBS and then washed twice with PBS. For isolating T cells, CD4$^+$ T cells were first enriched by magnetic-activated cell sorting beads (Miltenyi Biotec) and then stained with the indicated antibodies. The Becton Dickinson FACSVantage system and MoFlo sorter (DAKO Cytomation) were used for fluorescence detection and cell sorting.

**$T_H17$ differentiation *in vitro*.** Splenocytes from IL-17A–IRES–eGFP mice and C57BL/6 mice were incubated with CD4-microbeads and then positively selected through LS columns (Miltenyi Biotec). After enrichment, naive cells (CD4$^+$ CD25$^-$ CD62L$^{hi}$ CD44$^{low}$) were sorted by FACS as mentioned above. CD4$^+$ naive T cells were grown for 5 days at $10^6$ cells ml$^{-1}$ with plate-bound anti-CD3 (5 μg ml$^{-1}$) and soluble anti-CD28 (2 μg ml$^{-1}$) in medium (Bruff's medium supplemented with 10% FCS, L-glutamine, penicillin and streptomycin) under $T_H17$ conditions (TGF-β, IL-6, IL-23, anti-IFN-γ, anti-IL4). IL-17A (eGFP) expression was determined by flow cytometry.

**Multiphoton imaging.** The small intestine (duodenum) from an IL-17A–eGFP × Foxp3–mRFP double reporter mouse treated with CD3-specific antibody was mounted on a glass slide in a chamber consisting of a silicone isolator (20 mm diameter × 0.5 mm, Electron Microscopy Sciences). The tissue was immersed in PBS and covered by a glass coverslip. An Olympus BX50WI microscope equipped with a ×20x, numerical aperture 0.95 Olympus objective and a LaVision TriMScope Multiphoton System controlled by Imspector Software (LaVision Biotec) was used to collect images. For excitation, a Coherent Chameleon Ti:Sapphire laser was tuned to 960 nm. Images of 300 × 300 μm size were recorded at a resolution of 1,024 × 1,024 pixels with 1-μm *z*-spacing. Emitted light was collected with nondescanned detectors after having passed 435/90, 525/50 and 615/100 nm bandpass filters. Volocity software (Improvision) was used to create three-dimensional image stacks, and QuickTime Pro was used to generate image sequences.

***In vivo* T-cell stimulation and intestinal lymphocyte isolation.** Different mice in C57BL/6 background were injected with anti-CD3 (20 μg, 145 2C11)[34,35] intraperitoneally 1–3 times at an interval of 2 days between injections and killed 4 h after the final injection. For the controls, isotype control or PBS was injected. The intraepithelial lymphocytes (IEL) and lamina propria lymphocytes (LPL) were collected as described with some modifications[34]. In brief, small or large intestines were removed and Peyer's patches were dissected. The first 2 cm of the small intestine were considered as duodenum. Intestines were opened longitudinally and then were cut into strips 1 cm in length. Tissues were washed with Hank's buffered saline and incubated in the presence of 5 mM of EDTA at 37 °C for 30 min. The released cells were loaded onto a Percoll gradient and centrifuged. The cells between 40% and 100% Percoll were collected and used as intestinal epithelial lymphocytes. LPL were collected by digesting gut tissue, which was removed for IEL isolation as described above. The tissue was digested with collagenase IV (100 U, Sigma) at 37 °C for 1 h and loaded onto a Percoll gradient and centrifuged. The cells between 40% and 100% Percoll were collected and used as LPL.

For the lumen content isolation and analysis, mice were anesthetized using isoflurane. One ligation was made after the pylorus and a second one about 4–5 cm distal from the first ligation. A small incision without breaching the vessel proximal to the second ligation was made and 10 ml of pre-warmed PBS (2 ml min$^{-1}$) was injected using a syringe and a 27G1/2 needle. The fluids were collected in a Petri dish placed under the incision proximal to the second ligation. The collected fluids were incubated for 15 min in HBSS/ EDTA and then filtered through a 70 μm cell strainer before FACS analysis.

**Adoptive transfer of CD4$^+$ T cells.** CD4$^+$FoxP3$^+$ and the CD4$^+$FoxP3$^-$ T cells from the thymus or from the periphery of IL17A–eGFP × Foxp3–mRFP double reporter mice were collected and purified by magnetic-activated cell sorting (MACS; Miltenyi Biotec). After MACS enrichment, total CD4$^+$Foxp3$^+$ and CD4$^+$ FoxP3$^-$ T cells were FACS-sorted and $4 \times 10^6$ T cells were adoptively transferred (intravenously) into sub-lethally irradiated, sex-matched wild-type CD45.1$^+$ recipient mice. Four weeks after transfer, animals were injected with CD3-specific antibody (20 μg) and the small intestines were recovered and examined for eGFP and mRFP by FACS.

**Immunofluorescence microscopy.** Small intestines were removed from IL-17A–eGFP reporter mice and wild-type littermates after CD3-specific antibody treatment *in vivo*. Small intestines were fixed in 4% paraformaldehyde for 16 h. After two washes with PBS 20% sucrose solution was added. The 20% sucrose solution was replaced 16 h later with 30% sucrose solution. On the next day, the samples were washed and then snap-frozen in OCT and stored at −80 °C. Cryosections were cut at 12 μm on a Leica model CM1850 freezing microtome, applied to Superfrost Plus Gold slides (Fisher Scientific), air-dried, and PAP pen applied (Zymed Laboratories). Sections were blocked for 30 min at ambient temperature with serum-free protein block (Dako Cytomation) and were stained with PE–anti-CD4 (BD) and Alexa488–anti-GFP (Invitrogen) overnight at 4 °C. Samples were washed three times by immersing in PBS for 5 min and then mounted with Prolong gold mounting media with DAPI (Invitrogen). Sections were observed under dark field in independent fluorescence channels using an automated Olympus BX-61 microscope.

**Experimental autoimmune encephalomyelitis.** Mice were immunized subcutaneously with 250 μg of $MOG_{35-55}$ (Yale Keck facility) emulsified in CFA (BD Difco). Mice received 400 ng pertussis toxin (PTx, List Biological Laboratories) intraperitoneally at the time of immunization and 48 h later. Mice were checked for clinical symptoms daily, and signs were translated into clinical score as follows: 0, no detectable signs of EAE; 0.5, tail weakness; 1, complete tail paralysis; 2, partial hind limb paralysis; 2.5, unilateral complete hind limb paralysis; 3, complete

bilateral hind limb paralysis; 3.5, complete hind limb paralysis and partial forelimb paralysis; 4, total paralysis of forelimbs and hind limbs (mice with a score above 3.5 to be killed); 5, death. All animal experiments were conducted according to the IACUC policies.

**Cytokine assays.** Cytokines were quantified in plasma by ELISA (TGF-β1, Promega) or by Cytometric Bead Array (IL-6 and IL-17A, BD Bioscience) following the manufacturer's instructions. The plasma was obtained by centrifugation of blood collected on EDTA-coated tubes after cardiac puncture.

**Gene expression analysis.** Total RNA extracted (100 ng; RNeasy, Qiagen) from intestinal $rT_H17$ cells (from CD3-specific antibody-treated animals) or from pro-inflammatory $T_H17$ cells (from EAE-induced mice) were used to perform a genome-wide transcriptional profiling assay (GeneChip Mouse 1.0 ST Array, Affymetrix). Data was analysed with GeneSpring GX 10 (Agilent Technologies).

**Relative gene expression analysis.** RNA from cells/tissues was isolated with the RNeasy/QIAshredder purification system (Qiagen) in accordance with the manufacturer's protocol. RNA was subjected to reverse transcriptase with Superscript II (Invitrogen) with oligo(dT) primer in accordance with the manufacturer's protocol. cDNA was semi-quantified using commercially available primer/probe sets (Applied Biosystems) and analysed with the $\Delta\Delta C_t$ (change in cycle threshold) method. All results were normalized to *Hprt* quantified in parallel amplification reactions during each PCR quantification.

**Suppression assays.** CFSE (2 μM)-labelled $CD4^+CD25^-$ T cells (responder cells) were cultured in 96-well round bottom plates at $2 \times 10^4$ cells per well with $10^5$ irradiated APCs (spleenocytes MACS-depleted for $CD4^+$ and $CD8^+$ T cells) as feeder cells in the presence of $2 \times 10^4$ cells per well of FACS-sorted $CD4^+$IL-$17A^+Foxp3^-$ or $CD4^+$ IL–$17A^-Foxp3^+$ T cells. Cell cultures were stimulated with 2 μg $ml^{-1}$ of anti-CD3 antibody (2C11) in the presence or not of anti-TGF-β (1D11), anti-CTLA-4 (9H10) and anti-IL10R. After 4 days, cells were collected, stained and the CFSE signal was analysed by flow cytometry.

**Sepsis induced by infection and superantigen treatment:** Staphylococcus aureus (ATCC 14458, $SEB^+$ $TSST\text{-}1^-$) was injected intravenously into IL-17A–eGFP reporter mice ($10^8$ colony-forming units per mouse). Mice were killed 3 days after the injection, at a time when they displayed severe clinical symptoms of sepsis (weight loss, dehydration, lethargy) and the presence of $CD4^+IL17A^+$ T cells was tested in different organs (spleen, lymph node, small intestine) using FACS analysis. Similar experiments were done injecting the superantigens SEB and TSST-1. All of them were purchased from Toxin Technology. All superantigens were administered three times (0, 48, 96 h) intraperitoneally at 50 μg per mouse.

For the influenza A infection, mice were infected with $1 \times 10^4$ plaque-forming units of influenza A/PR8 (H1N1) virus via the intranasal route. Infection was performed by the intranasal application of 50 μl virus stock diluted in PBS (or an equal volume of PBS as a control) to mice that had been deeply anesthetized with anafane (Ivesco). Lungs and small intestines were harvested 3 and 5 days after infection for flow cytometry analysis.

**Peripheral blood mononuclear cells isolation and administration.** Human leukocytes were collected by leukapheresis of adult volunteer donors under a protocol approved by the Yale Human Investigations Committee. The peripheral blood mononuclear cells were isolated using Lymphocyte Separation Medium (Cappel) according to the manufacturer's instructions. The cells were stored in 10% DMSO/90% FBS at −196 °C and were thawed and washed before use. $Rag2^{-/-} \times \gamma c^{-/-}$ double knockout mice were reconstituted with $5 \times 10^7$ human peripheral blood mononuclear cells by intraperitoneally inoculation 2 weeks before anti-CD3 specific antibody treatment. The number of human T cells ($CD45^+CD4^+$) in the small intestine was evaluated by flow cytometry. Animals demonstrated no signs of graft-vs-host disease. Rare animals that failed to reconstitute with human T cells were, by prior design, excluded from analysis.

**Endoscopic procedure.** Colonoscopy was performed in a blinded fashion for colitis scoring using the Coloview system (Karl Storz, Germany). Briefly: colitis scoring was based on granularity of mucosal surface, stool consistence, vascular pattern, translucency of the colon and fibrin visible (0–3 points for each).

**Statistical analysis.** Where indicated, the Student *t* test for non-paired data and the Mann–Whitney *U* test were used to calculate statistical significance for differences in a particular measurement between different groups. A *P*-value of less than 0.05 was considered significant.


30. Bettelli, E. *et al.* Myelin oligodendrocyte glycoprotein-specific T cell receptor transgenic mice develop spontaneous autoimmune optic neuritis. *J. Exp. Med.* **197,** 1073–1081 (2003).
31. Wan, Y. Y. & Flavell, R. A. Identifying Foxp3-expressing suppressor T cells with a bicistronic reporter. *Proc. Natl Acad. Sci. USA* **102,** 5126–5131 (2005).
32. Nakae, S. *et al.* Antigen-specific T cell sensitization is impaired in IL-17-deficient mice, causing suppression of allergic cellular and humoral responses. *Immunity* **17,** 375–387 (2002).
33. Ye, P. *et al.* Requirement of interleukin 17 receptor signaling for lung CXC chemokine and granulocyte colony-stimulating factor expression, neutrophil recruitment, and host defense. *J. Exp. Med.* **194,** 519–528 (2001).
34. Kamanaka, M. *et al.* Expression of interleukin-10 in intestinal lymphocytes detected by an interleukin-10 reporter knockin *tiger* mouse. *Immunity* **25,** 941–952 (2006).
35. Alegre, M. L. *et al.* An anti-murine CD3 monoclonal antibody with a low affinity for Fc gamma receptors suppresses transplantation responses while minimizing acute toxicity and immunogenicity. *J. Immunol.* **155,** 1544–1555 (1995).